Proceedings of HT-FED04
2004 ASME Heat Transfer/Fluids Engineering Summer Conference
July 11-15, 2004, Charlotte, North Carolina USA

HT-FED04-56242

EFFECTIVE THERMAL CONDUCTIVITY OF FULLY-SATURATED HIGH POROSITY METAL FOAM

Eric N. Schmierer
Tritium Science and Engineering Group, MS C348
Los Alamos National Laboratory
Los Alamos, New Mexico 87545, USA

Jason Paquette
Mechanical Engineering Department
University of Nevada at Reno
Reno, Nevada 89557, USA

Arsalan Razani
Mechanical Engineering Department
The University of New Mexico
Albuquerque, New Mexico 87131, USA

Kwang. J. Kim
Mechanical Engineering Department
University of Nevada at Reno
Reno, Nevada 89557, USA

Keywords: metal foam, effective thermal conductivity, FEA, porous material

ABSTRACT

Geometric models are used to simplify the complex, three-dimensional geometry of metal foams for calculations of effective thermal conductivity. The first is based on a conventional three-dimensional cubic lattice and the second is a tetrakaidecahedronal model. The models consist of interconnecting ligaments with a spherical node at their intersections. The geometry of the foam is determined based on two dimensionless parameters: 1) the porosity and 2) the product of the specific surface area of the foam and the length of the interconnecting ligaments. A free parameter represents the size of the lumps at the ligament interconnections. It is shown that the remaining unknown geometric parameters of the models can be obtained as a solution of a cubic equation that has only one acceptable solution. From the cubic lattice model, a one-dimensional heat conduction analytical model is used to find the effective thermal conductivity of fully saturated metal foam. A three-dimensional finite element calculation of the effective thermal conductivity for the cubic lattice is then compared to the one-dimensional model. In the case of the tetrakaidecahedronal model, a similar three-dimensional finite element calculation is performed to find the effective thermal conductivity. Anisotropy of the models is explored. The results of the models are compared with experimental results from this study and the literature to substantiate their accuracy. The experimental results are reported for fully saturated aluminum metal foam in air, water, and oil. Results show that both the cubic lattice model, which is less complex, and the tetrakaidecahedronal model can both be used to represent one-dimensional effective thermal conductivity. Finally, the dimensionless surface areas for each geometric model are compared. The models produce significantly different surface areas, and therefore do not both represent the density and specific surface area of foam accurately.

INTRODUCTION

The thermal conductivity of fully saturated porous matrices is important in several areas of science and engineering [1]. Several authors have reported experimental studies of effective thermal conductivity of general amorphous multiphase systems [1-3]. The evaluation of stagnant thermal conductivity of multi-component matrices with a periodic structure has also been the subject of several studies both in two and three dimensions [4-6]. Specifically for high porosity metal foam, various ideal representations of the complex, three-dimensional geometry have been used for calculation of effective thermal conductivity. Saturated high porosity metal foam has been studied this way by several authors semi-analytically [7-9]. These studies developed analytical solutions for effective thermal conductivity and used experimental data to determine a free geometric parameter. Application for these works was mixed conduction and convection heat transfer applications. Experimental investigation of effective thermal conductivity of high porosity saturated metal foam has been studied as well for the range of common foam parameters [7, 9, 10]. The authors are not aware of any numerical analysis of the thermal conductivity or study into its anisotropy for high porosity open-celled metal foam.

In this study, two ideal representations of high porosity metal foam are investigated, a cubic and tetrakaidecahedronal lattice. The geometry of the foam is determined based on the

relative density and dimensionless specific surface area. A free parameter, that represents the size of the lumps at the ligament interconnections, is used to match the model porosity and ligament diameter. It is shown that the remaining unknown geometric parameters of the models can be obtained.

No prior experimentally-based parameters other than the basic foam characterizing parameters are used to develop the geometric models for the foam. From the cubic lattice model, a one-dimensional heat conduction analytical model is developed. It is used to find the effective thermal conductivity of fully saturated metal foam for parameter exploration and verification of a three-dimensional finite element calculations.

Experimental results are reported for fully saturated aluminum metal foam in air, water, and oil. The results of the finite element calculations are compared with the results reported in the literature. The thermal conductivity results of the two models are compared to data to determine the applicability of the models for stagnant heat conduction. The resulting dimensionless surface area is also compared between models to evaluate their applicability to convection and multi-dimensional heat transfer analysis.

NOMENCLATURE

D	spherical node diameter
L_{II}	length of sample in thermal conductivity experiment
L_{III}	length between the 1st and 4th thermocouple of experimental apparatus
P	dimensionless porous foam matrix, δS_v
PPI	common designation for pores per inch (1/in.)
R_1	the resistance due to solid vertical ligament
R_2	the resistance due to the fluid
R_3	resistance due to the solid part of horizontal ligaments
R_4	resistance due to the fluid part of horizontal ligaments
R_5	resistance due to the solid part of the spherical node
R_6	resistance due to the fluid part of the spherical node
S	surface area of ligaments in cubic lattice, m^2
S_v	specific surface area, (1/m)
T_i	steady state temperature of the ith thermocouple
V_m	volume of the ligaments, m^3
d_f	ligament diameter, m
d_p	pore diameter, m
f	parameter defined by Eq. (1)
g	parameter defined by Eq. (1)
h	parameter defined by Eq. (2)
h_c	contact conductance in experimental setup ($W/m^2/K$)
k_{eff}	foam matrix effective thermal conductivity (W/m/K)
k_f	thermal conductivity of fluid, (W/m/K)
k_I	reference thermal conductivity for experiment
k_s	thermal conductivity of solid material (W/m/K)
k_{water}	thermal conductivity of water, (W/m/K)
m	parameter defined by Eq. (2)
u	ligament diameter to length ratio
β	node size parameter
Δ	function of β
Δx	length of conduction path in FEA model
Φ	foam cell diameter
δ	length of ligament
ε	porosity
φ	pore density (pores/m)
λ_c	effective length of horizontal cylindrical ligaments
λ_s	effective length of spherical node not included in R_1

FORMULATION OF GEOMETRIC MODELS

Two geometric models were investigated. The first model consists of a three-dimensional cubic lattice (Cubic). In the second model a tetrakaidecahedronal lattice (TetraK), which is generally accepted as a more representative model of the foam [11]. Both structures are space filling, and they are shown in Fig. 1 and Fig. 2.

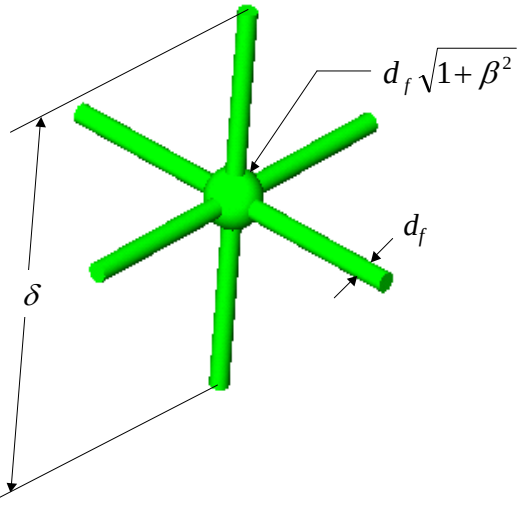

Figure 1. Cubic lattice (Cubic) model and parameters

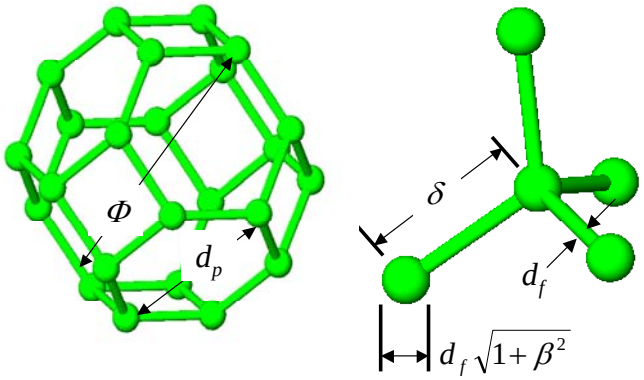

Figure 2. Tetrakaidecahedronal lattice (TetraK) model

The actual structure of the foam matrix is a complex one with a lump of material at the ligament intersection. In both models we assume that a spherical node is formed at the intersection. The basic parameters representing the metal foams are the porosity, ε, specific surface area, S_v, ligament diameter, d_f, and the ligament length, δ, and a node size parameter, β. These parameters must be chosen such that the model characterizes the metal foam as close as possible. An additional parameter usually reported by manufacturers of the open-celled metal foam is the pore density, φ (pores per unit length). This is the measure of the periodicity of the structure,

whereas the previous parameters describe the unit cell of diameter Φ.

Using the space filling properties of the two geometric models, a relation between the basic parameters in terms of dimensionless numbers can be written as,

$$u^3 - f(\beta)u^2 + g(\beta)(1-\varepsilon) = 0 \quad (1)$$

$$u^2 - h(\beta)u + m(\beta)P = 0 \quad (2)$$

where,

$$u = \frac{d_f}{\delta} \qquad and \qquad P = S_v\delta \quad (3)$$

and f(β), g(β), h(β), and m(β) are functions of node parameter β. β is defined in terms of the diameter of the spherical node, D, and ligament diameter, d_f by,

$$\beta = \sqrt{(D/d_f)^2 - 1} \quad (4)$$

Depending on the model, a constraint on the node parameter must be enforced to assure that the exposed surface area at the node is positive and the node volume is larger than the volume of the connecting ligaments at the node. Table 1 and Table 2 present the functions f, g, h and m as a function of β, where the functions X and Y are given respectively by,

$$X = 8(1+\beta^2)^{1.5} - 4(\sqrt{1+\beta^2} - \beta)[3 + (\sqrt{1+\beta^2} - \beta)^2] \quad (5)$$

$$Y = (\sqrt{1+\beta^2} - \beta)[3 + (\sqrt{1+\beta^2} - \beta)^2] \quad (6)$$

Table 1. Functions f(β), g(β), h(β), and m(β) used in Eq. (1) and Eq. (2) for the Cubic model

f(β)	$1/[\beta - (2/9)(1+\beta^2)^{1.5} + Y/6]$
g(β)	$1/\pi[3\beta/4 - (1/6)(1+\beta^2)^{1.5} + Y/8]$
h(β)	$1/[\beta - \beta\sqrt{1+\beta^2} + 2(1+\beta^2)/3]$
m(β)	$1/\pi[3\beta - 3\beta\sqrt{1+\beta^2} + 2(1+\beta^2)]$

Table 2. Functions f(β), g(β), h(β), and m(β) used in Eq. (1) and Eq. (2) for the TetraK model

f(β)	$1/(\beta - X/24)$
g(β)	$8\sqrt{2}/[\pi(3\beta - X/8)]$
h(β)	$2/[(1+\beta)^2 - 2\beta\sqrt{1+\beta^2}]$
m(β)	$4\sqrt{2}/3\pi[(1+\beta)^2 - 2\beta\sqrt{1+\beta^2}]$

The solution of Eq. (1) has one acceptable root for a given parameter set. When the value Δ, given by

$$\Delta = g(\beta)\left[g(\beta)(1-\varepsilon)/4 - f(\beta)^3/27\right] \quad (7)$$

is less than zero, there are three real roots of Eq. (1) where only one is physically acceptable. In general, this root can be written as,

$$u = (2/3)\left[\cos\left(\frac{1}{3}\arccos\left(1 - \frac{27(1-\varepsilon)g(\beta)}{2f(\beta)^3}\right) + \theta\right)\right] + f(\beta)/3 \quad (8)$$

For the case of the tetrakaidecahedronal lattice and the practical range of β when f(β) > 0 (β < 1.304), then θ = 4π/3 and when f(β) < 0 (β > 1.304), then θ = 2π/3. It should be pointed out that for the case of Δ > 0 the only one acceptable root of Eq. (1) is not in most cases in the practical range of application and it is not given here.

Once u is obtained by assuming a value for β, Eq. (2) gives the dimensionless surface parameter, P. In order to obtain quantitative values for d_f and S_v, the ligament length must be known. The ligament length, δ, is simply a scaling of the unit cell size, which relates to the pore density. For the cubic lattice this relation is simply δ = 1/φ and for the tetrakaidecahedronal unit cell, δ = 0.658/φ. With these relations and Eq. (3), the geometry of the foam can be completely defined.

It should be pointed out that there are experimental evidences that the cross-section of the ligaments connecting the nodes are, in general, a function of porosity and change from circular for ε = 0.85 to an inner concave triangle at ε = 0.97 [7]. In this work, the functions f(β), g(β), h(β), and m(β) are only functions of the node parameter and porosity, and this cross-section variation with porosity is neglected.

EFFECTIVE THERMAL CONDUCTIVITY

Using the geometric models determined for the two lattice structures, the effective thermal conductivity can now be determined. A one-dimensional analytical solution is first derived for the cubic model. The effective thermal conductivity results from this model are compared to a numerical solution for this problem to verify the numerical method. The effective thermal conductivity is then determined numerically for the tetrakaidecahedronal model. Finally, experimental results for thermal conductivity are obtained and compared to the numerical results for both.

Cubic One-Dimensional Analytical Solution

Using the geometry for the cubic model given in Fig. 1, the total thermal resistance for the saturated unit lattice composed of two phases (solid and fluid) can be calculated. The thermal resistance, assuming one dimensional heat transfer, is the combination of four parallel thermal resistances. One is a thermal resistance due to the solid vertical ligament. The second thermal resistance is through the fluid parallel to the solid ligament. The third thermal resistance is a combination of three resistances in series: first through fluid, then through the four horizontal ligaments and through the fluid again. The fourth thermal resistance is through the fluid, then through the surrounding node at the ligaments' cross-section and through the fluid again.

The effective thermal conductivity ratio for the fully saturated foam matrix can be written as,

$$\frac{k_{eff}}{k_f} = \frac{1}{R_1} + \frac{1}{R_2} + \frac{1}{R_3 + R_4} + \frac{1}{R_5 + R_6} \tag{9}$$

where R_1 is the non-dimensional resistance due to the solid vertical ligament, R_2 is the resistance due to the fluid, R_3 and R_4 are the series resistances due to the solid and fluid for the horizontal ligament sections, and R_5 and R_6 are the series resistances for the solid and fluid through the node minus the vertical ligament. Figure 3 is a schematic showing the regions for the one-dimensional calculation.

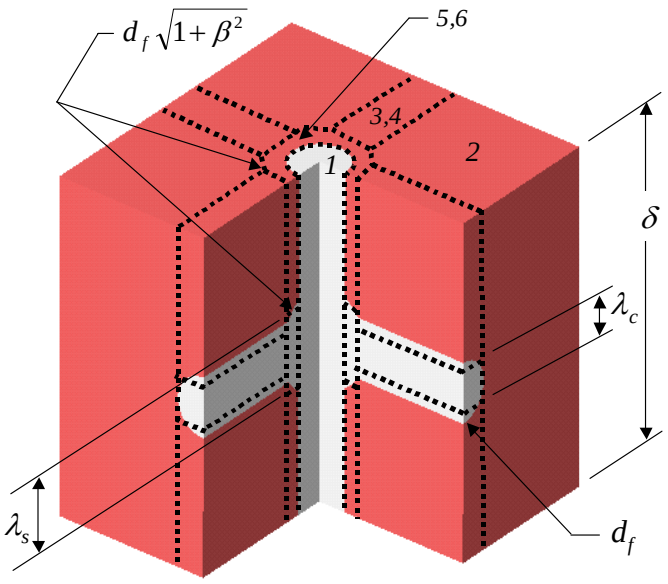

Figure 3. Schematic showing regions used in derivation of the Cubic 1-D analytical solution

To evaluate the resistances, the average heat conduction path through the horizontal cylindrical ligaments, region 3 and 4, and spherical node, region 5 and 6, were derived first,

$$\lambda_c = \frac{\pi}{2} d_f \tag{10}$$

$$\lambda_s = \frac{2\pi d_f}{3} \frac{2\sqrt{1+\beta^2} + 2\beta^2\sqrt{1+\beta^2} - 3\beta - \beta^3}{\left(\pi - 2\beta - 2\beta^2\right)} \tag{11}$$

where λ_c is the average heat conduction path through the horizontal cylindrical ligaments, and λ_s is for the average heat conduction path of the spherical node. It should be pointed out that the equivalent spherical node excludes the solid vertical ligament passing through the node.

These dimensionless thermal resistances are given for the Cubic 1-D model by,

$$R_1 = \frac{4}{\pi u^2} \frac{k_f}{k_s} \tag{12}$$

$$R_2 = \frac{1}{\left(1-u^2\right) - \frac{u^2}{2}(\beta - 1)^2} \tag{13}$$

$$R_3 = \frac{\pi}{8(1-\beta u)} \frac{k_f}{k_s} \tag{14}$$

$$R_4 = \frac{4 - \pi u}{8u(1-\beta u)} \tag{15}$$

$$R_5 = \frac{8\pi\left(2\sqrt{1+\beta^2} + 2\beta^2\sqrt{1+\beta^2} - 3\beta - 3\beta^3\right)}{u\left[6\beta(1+\beta) - 3\pi\right]\left(\pi - 2\beta - 2\beta^2\right)} \frac{k_f}{k_s} \tag{16}$$

$$R_6 = \frac{-24\beta(1-\beta) + 12\pi - 8\pi u\left(2\sqrt{1+\beta^2} + 2\beta^2\sqrt{1+\beta^2} - 3\beta - 3\beta^3\right)}{3u^2\left(\pi - 2\beta - 2\beta^2\right)^2} \tag{17}$$

Therefore, the effective thermal conductivity ratio of the combined matrix is given by Eq. (9) and can be written as a function of k_s/k_f, u, and β.

Numerical Effective Thermal Conductivity Models

The first step in investigating effective thermal conductivity of the two structures numerically was development of the FEA models. Unigraphics solid modeling software [12] was used to create solid geometry that was then exported to COSMOS/M and DesignSTAR [13] for analysis. The unit cell side lengths were fixed. Temperature boundary conditions were applied at x_i and $x_i + \Delta x_i$, where i is the direction of heat flux. Spatial convergence testing was performed over a large range of k_s/k_f for $\varepsilon = 0.85$ to determine the mesh refinement necessary on the boundary and the solid/fluid interfaces. There was less than 4% variation between what was considered a coarse mesh and the final mesh used. The mesh sizing used on each boundary and the solid/fluid interface was the same. Figure 4 shows the final model used for the Cubic FEA model.

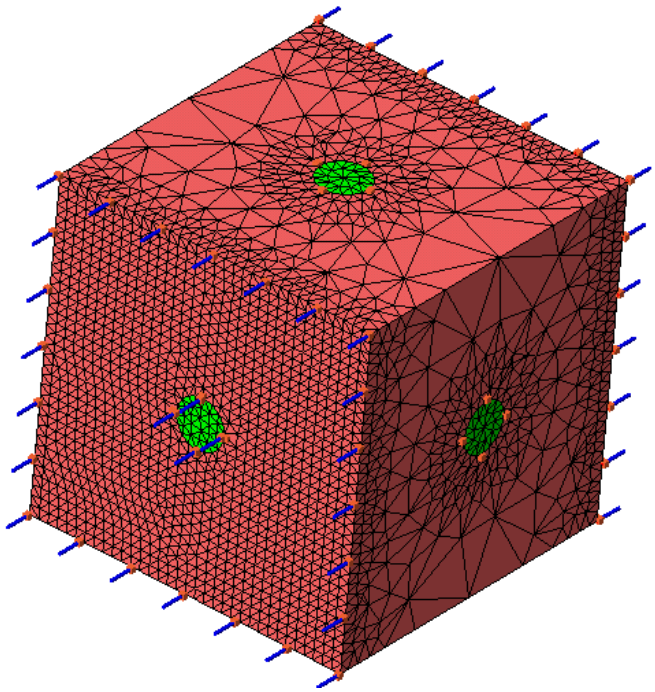

Figure 4. Final Cubic FEA model (ε = 0.95, β = 1)

For a given set of geometric parameters (ε, β, k_s/k_f), the average nodal heat flux is calculated, and the effective thermal conductivity was calculated using the following equation,

$$k_{eff,i} = \frac{q_i \Delta x_i}{\Delta T}, \; i = \text{x,y, z,} \tag{18}$$

The model for the TetraK FEA model was developed similarly (Fig. 5). The model consists of 1/16 of a tetrakaidecahedron, presented by Boomsma and Poulikakos [8].

In order to quantitatively compare the models to each other some assumptions have to be made regarding their equivalency. When considering the geometric parameters, in additional to constant density between models, three scenarios were considered: constant d_f, constant d_p, and constant pore area, A_p. These three scenarios produce different geometry if the ligament length, δ, is allowed to change. However, if the geometric parameters are normalized by δ then the three scenarios result in the same geometry comparison. That is, following calculation of parameters using Eqs. (1-8) and normalization with the resulting ligament length, the three scenarios result in the same FEA models.

Both the TetraK and Cubic FEA models were explored for anisotropy of the thermal conductivity. An additional cubic lattice model was required to simulate this with the axis of the ligaments rotated about the three axes by 45°, shown in full in Fig. 6 and just the ligaments in Fig. 7.

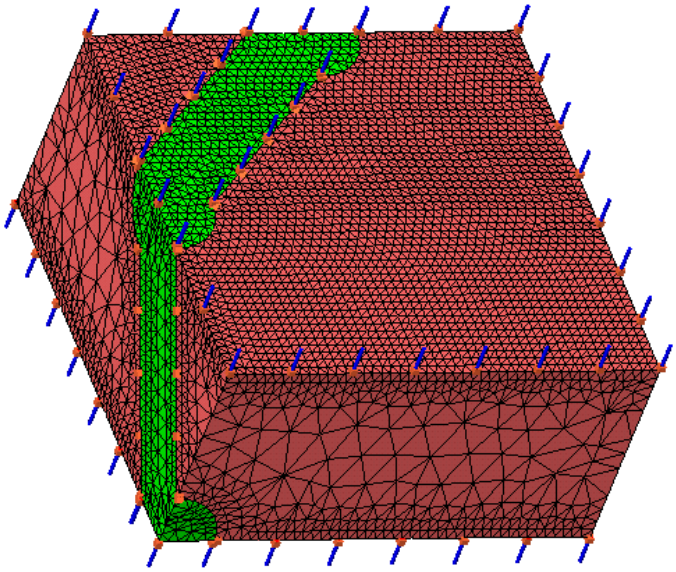

Figure 5. Tetrakaidecahedronal (TetraK) FEA model (ε = 0.95, β = 1)

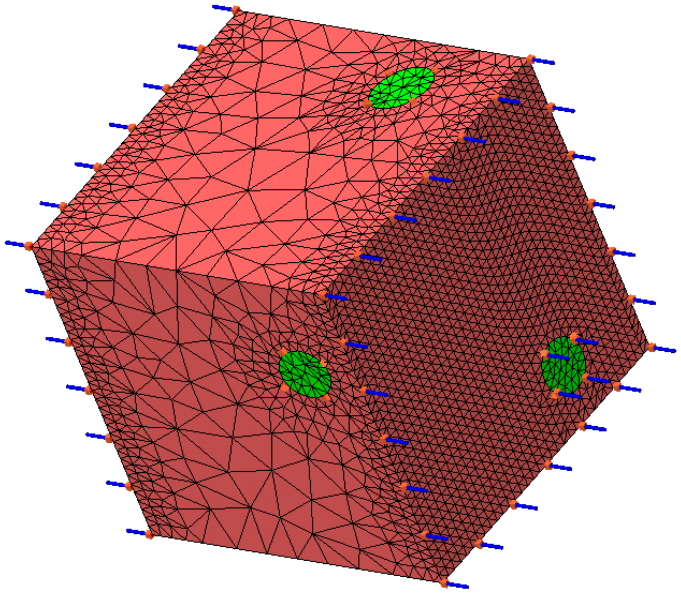

Figure 6. Cubic Rotated FEA model (ε = 0.95, β = 1)

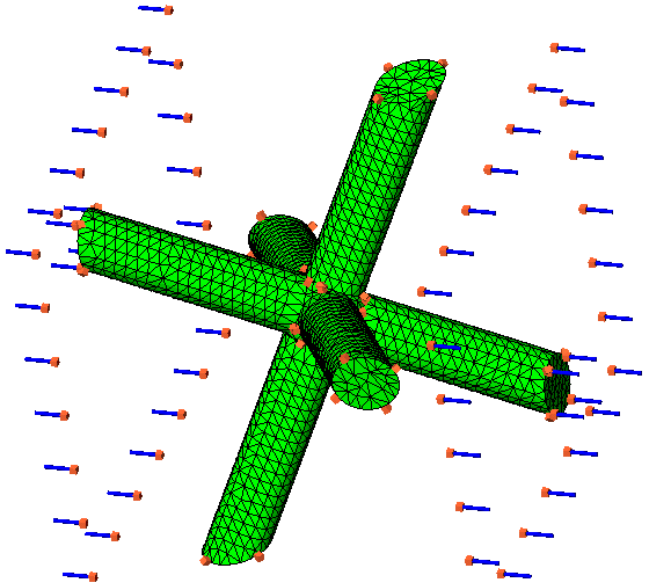

Figure 7. Cubic Rotated FEA solid only portion showing orientation of ligaments (ε = 0.95, β = 1)

Experimental Investigation

Through the use of the experimental apparatus shown in Fig. 8, the experimental thermal conductivity of the porous foam matrix was determined. The apparatus consists of a heating element that uses 6-volts to introduce a steady source of heat to the sample. Heat is conducted through the test section (with a one-dimensional heat transfer assumption) towards a copper heat sink cooled with flowing water. This relies on the temperature gradient through a 9.53 mm diameter 304 stainless steel meter bar to determine the heat flux. Type T thermocouples are located in the center of the meter bar, with T_4 and T_5 located 0.25 mm from the contact face.

In order to measure the thermal conductivity of the porous foam matrix within a fluid medium, a modification was made to the apparatus used by Kim [14]. A capsule was made to contain a sample of the porous foam matrix as well as a fluid.

The capsule was an acrylic cylinder with a steel top and bottom. The bottom was sealed tight, leaving the top of the capsule open to place the sample and the fluid in. After placing the steel top under a 50-psia pressure exerted by the micrometer allowing for an adequate seal. The space outside of the capsule was subsequently evacuated.

The various fluids used in these experiments were air (12 psia), water, and oil. The metal foam used in the experiment was 6101 aluminum Duocell foam [15] with a pore density of 20 PPI and a porosity of 0.95. The foam and fluid parameters are summarized in Table 3.

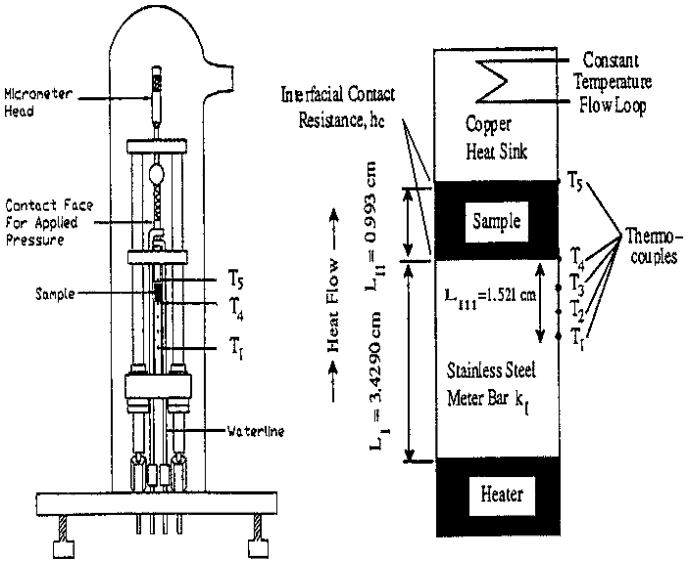

Figure 8. Schematic of experimental apparatus [14]

Table 3. Experimental fluid and foam parameters

k Aluminum (W/m/K)	218
Foam porosity	0.95
Foam pore density (pores/in.)	20
k Air (W/m/K)	0.0269
k Oil (W/m/K)	0.1450
k Water (W/m/K)	0.6248

The experiment was run until steady state temperatures were attained, which was approximately two hours. The various thermocouples placed on the apparatus allow for the determination of the effective thermal conductivity of the sample through the use of Eq. (19).

$$k_{eff} = \frac{L_{II} k_I \left(\frac{T_4 - T_1}{L_{III}} \right)}{T_5 - T_4 - 2\frac{k_I}{h_c}\left(\frac{T_4 - T_1}{L_{III}} \right)} \qquad (19)$$

Equation (19) neglects conduction through the acrylic material and any temperature drop through the steel ends of the sample holder. The general uncertainty analysis of the experiment yielded an uncertainty in the experimental k_{eff} of approximately 20% for air, which was the worst case. The dominating term in the uncertainty equation was the contact resistance term between the sample and the steel plate.

RESULTS AND DISCUSSION

Cubic 1-D to Cubic FEA Comparison

The Cubic 1-D analytical results from Eq. (9) for k_{eff}/k_f were compared to the numerical results for the Cubic FEA model. Figure 9 shows the ratio of the Cubic 1-D to Cubic FEA k_s/k_f. The variation between the one-dimensional analytical model and the FEA model increases up to about 23% for large k_s/k_f. This was higher than expected and does not trend as expected with porosity. Given the results of the spatial convergence tests it is believed that these are physical difference between the models, however further investigation into this is warranted.

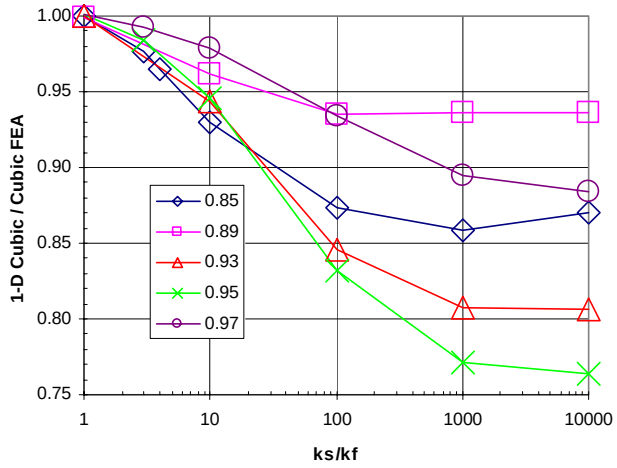

Figure 9. Ratio of Cubic 1-D to Cubic FEA results for k_{eff}/k_f for varying porosity

Effective Thermal Conductivity Anisotropy

The effective thermal conductivity of the Cubic FEA and Cubic Rotated FEA models were compared next. Their ratio is plotted in Figure 10. The ratio between the TetraK FEA z and x directions are plotted in Fig. 11 for the porosity extremes. The variation between the rotated and non-rotated Cubic and the directional TetraK was largest for the smallest porosity, which was expected. The maximum variations were approximately 25% and 5% respectively.

Cubic FEA and TetraK FEA Model Comparison

The effective thermal conductivity of fluid-saturated metal foam k_{eff}/k_f, for the cubic and tetrakaidecahedron models are compared versus k_s/k_f in Fig. 12 for $\beta = 1$ and the extremes of the density range considered. The ratio of the results compare well for low k_s/k_f and are a maximum of about 11% for the highest density. The average thermal conductivity was determined by weighting the respective directional values using Eqs. (20) and (21).

$$\frac{k_{eff}}{k_s}(aveTetraK) = \frac{2\frac{k_{eff}}{k_s}(TetraK\_x) + \frac{k_{eff}}{k_s}(aveTetraK\_z)}{3} \qquad (20)$$

$$\frac{k_{eff}}{k_s}(aveCubic) = \frac{\frac{k_{eff}}{k_s}(Cubic) + \frac{k_{eff}}{k_s}(CubicRotated)}{2} \qquad (21)$$

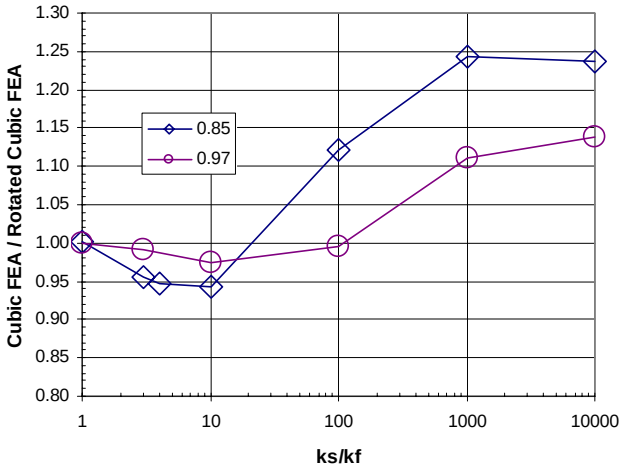

Figure 10. Ratio of Cubic FEA to Cubic Rotated FEA k_{eff}/k_f for porosity range extremes

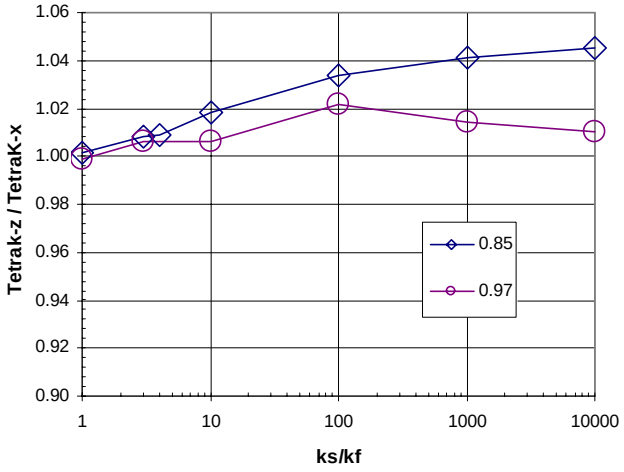

Figure 11. Ratio of TetraK-z to TetraK-x k_{eff}/k_f for porosity range extremes

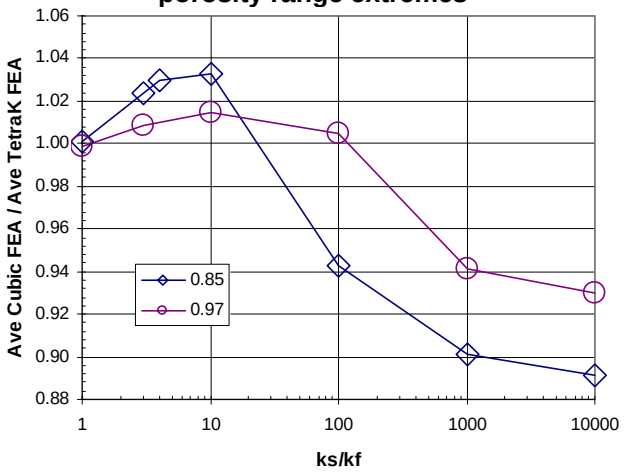

Figure 12. Ratio of average Cubic to average TetraK k_{eff}/k_f for porosity range extremes

Table 4. Normalized k_{eff} results and variation to results from the present experiment

Fluid	Experi-mental k_{eff}/k_f	Cubic FEA k_{eff}/k_f	TetraK FEA k_{eff}/k_f	BCM [7] k_{eff}/k_f	Cubic Var.	TetraK Var.	BCM Var.
Air	131.4	164.9	169.5	148.8	20%	22%	12%
Oil	27.4	31.5	32.2		13%	15%	
Water	7.8	8.0	8.3	7.9	3%	6%	2%

Experimental Data and FEA Model Comparison

The average thermal conductivity of each fluid was determined based on the average fluid temperature during an experiment (34.8°C). Figure 13 compares the experimental data to the two model calculations and Fig. 14 is the variation between the experimental data and the FEA models. Data from Calmidi and Mahajan [9] was shown also in Fig. 13. Table 4 is a summary of the results.

Both the average Cubic FEA and TetraK FEA model results compare well with the experiment for low k_s/k_f and the data from Calmidi and Mahajan [9]. The variation of each model is approximately the same and increases with k_s/k_f. Based on the uncertainly analysis performed, it's believed that a significant portion of the error in the experiment is due to the contact resistance between the sample and the apparatus, which is exasperated at the higher k_s/k_f ratio.

To address the large uncertainty in the experimental data, the experiment is being redesigned to minimize the contact resistance effects. Additionally, the direction of the heat flow vector will be inverted to minimize natural convection within the sample fluid.

It is interesting to note that, the models used in this study show that the effective thermal conductivity ratio only depends on the dimensionless ligament diameter to ligament length ratio, u. This parameter is only a function of porosity of the porous foam matrix. This is consistent with results from Calmidi and Mahajan [9].

The results indicate that the cubic and the tetrakaidecahedronal lattice models perform the same for determining the effective thermal conductivity of stagnant saturated metal foam. Figure 15 is a plot of the k_{eff}/k_f versus k_s/k_f using the TetraK FEA model for use with future applications. Shown also in Fig. 15 is a simple power function of the form:

$$\frac{k_{eff}}{k_f} = C(1-\varepsilon)k_s \qquad (22)$$

where C = 0.44. This represents the foam-only contribution to the effective thermal conductivity. This shows that for k_s/k_f less than 1000-2000 the fluid contribution must be considered also.

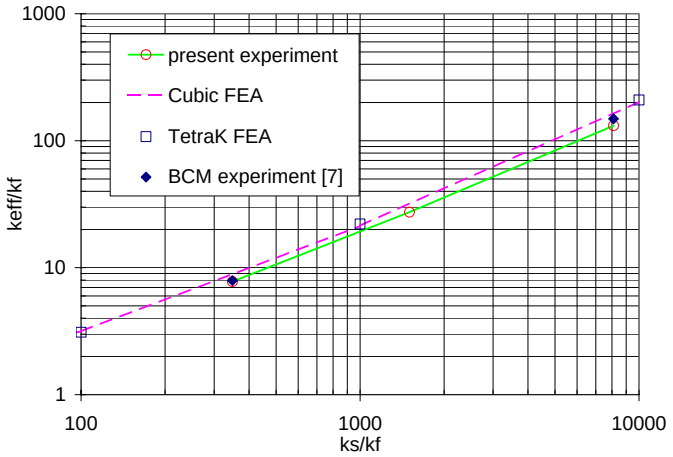

Figure 13. Experimental data compared to FEA models

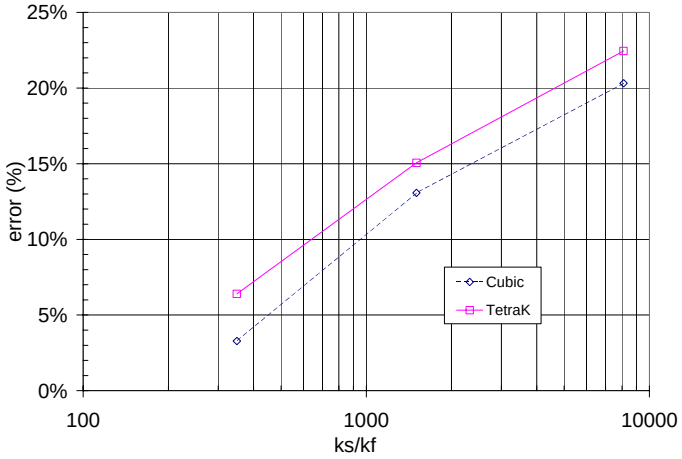

Figure 14. Variation between model and experimental data as a function of k_s/k_f

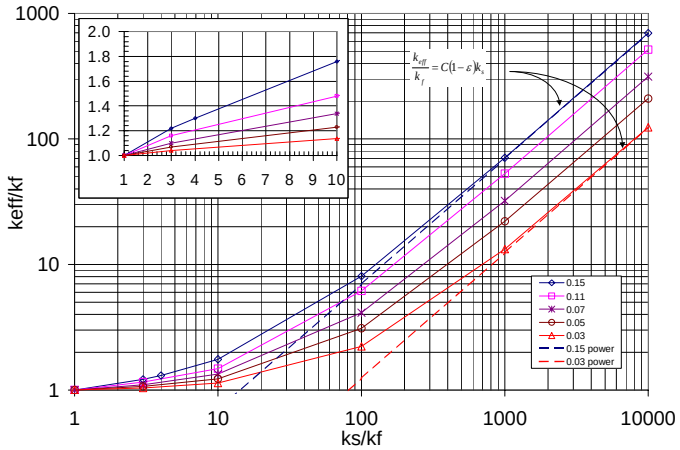

Figure 15. TetraK model predictions for k_{eff}/k_f for different metal foam densities

Model Surface Area Comparisons

With u determined for the two models from Eq. (8), the resulting dimensionless surface area was calculated using Eq. (2). These are shown in Table 5 for P and the ratio of the two model calculations. Figure 16 shows the values versus porosity. The results show that there is significant difference between the models for the dimensionless specific surface area prediction, a factor of 1.7 to 2.0. Therefore, use of the both models may not be appropriate for convection heat transfer applications, since the interfacial area will govern this mode of heat transfer. To quantitatively evaluate the two models, actual surface area data is required as a function of the foam porosity and pore density, which does not exist experimentally. Another factor that will affect the actual surface area is the shape of the ligament cross-section, which has been shown to vary with density [7]. The value of β does not significantly affect P for the Cubic model, however, it is more significant for the TetraK model. This is attributed to the two additional ligaments that the Cubic model has for each node, reducing the portion of the surface area that is in the node.

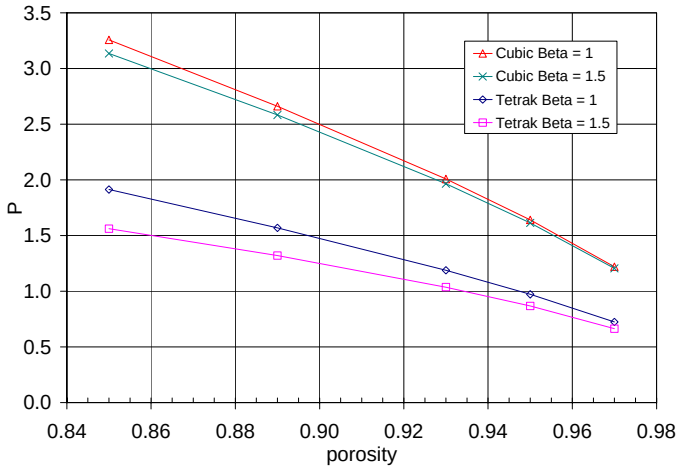

Figure 16. P for the two models at β=1 and β=1.5

Table 5. Dimensionless parameters u and P from Eqs. 1-8 compared for different β and porosity

β	ε	u,c / u,t	P,c / P,t
1	0.85	0.61	1.70
1	0.89	0.61	1.70
1	0.93	0.60	1.69
1	0.95	0.60	1.69
1	0.97	0.60	1.69
1.5	0.85	0.66	2.01
1.5	0.89	0.65	1.96
1.5	0.93	0.64	1.90
1.5	0.95	0.63	1.86
1.5	0.97	0.62	1.82

CONCLUSIONS

A cubic and tetrakaidecahedronal three-dimensional model were used to replace the complex structure of high porosity metal foam to evaluate effective thermal conductivity with the finite element method. The porosity and specific surface area of the foam were determined in terms of dimensionless parameters convenient for parametric studies of both models. FEA of the cubic model was compared to a one-dimensional analytic solution, which indicated some difference, however provides a less complex model. The experimental measurements of effective thermal conductivity were obtained with good agreement with other data in the literature and with the results of the two FEA models for low k_s/k_f. The error

increased up to 20% for the large k_s/k_f data point. Contact conductance is attributed with the majority of the error, and the experimental apparatus is being redesigned. Both models varied similarly from experimental data indicating that either geometric model is valid for representing conduction heat transfer only. The finite element modeling demonstrated the capability for calculating effective thermal conductivity of complex geometries or expanded unit cells. The resulting dimensionless specific areas were compared for each model for constant density, and they produce significantly different dimensionless surface areas. Therefore both will not represent mixed heat transfer accurately. More investigation into affect of the node parameter and ligament cross-sectional shape on surface area is required, and ultimately experimental work on surface area is required to determine which model is more appropriate in this regard.

ACKNOWLEDGMENTS

The authors gratefully acknowledge Mr. Bryan Leyda of ERG Materials and Aerospace Corporation for the informative discussions and for providing the sample used in the experiments.

REFERENCES

[1] Kaviany, M., 1999, *Principle of Heat Transfer in Porous Media*, 2nd ed., New York, Springer.
[2] Nozad, I., R. G. Carbonell, and S. Whitaker, 1985, "Heat-Conduction in Multiphase Systems .1. Theory and Experiment for 2-Phase Systems," Chemical Engineering Science, **40**, pp. 843-855.
[3] Nozad, I., R. G. Carbonell, and S. Whitaker, 1985, "Heat-Conduction in Multiphase Systems .2. Experimental-Method and Results for 3-Phase Systems," Chemical Engineering Science, **40**, pp. 857-863.
[4] Hsu, C., P. Cheng, and K. Wong, 1995, "Modified Zehner-Schlunder Models for Stagnant Thermal-Conductivity of Porous Media," International Journal of Heat and Mass Transfer, **37**, pp. 2751-2759.
[5] Hsu, C. T., P. Cheng, and K. W. Wong, 1995, "A Lumped-Parameter Model for Stagnant Thermal-Conductivity of Spatially Periodic Porous-Media," Journal of Heat Transfer-Transactions of the ASME, **117**, pp. 264-269.
[6] Dul'nev, G. N., 1965, "Heat Transfer through Solid Disperse Systems," Journal of Engineering Physics, **9**, pp. 275-278.
[7] Bhattacharya, A., V. V. Calmidi, and R. L. Mahajan, 2002, "Thermophysical Properties of High Porosity Metal Foams," International Journal of Heat and Mass Transfer, **45**, pp. 1017-1031.
[8] Boomsma, K. and D. Poulikakos, 2001, "On the Effective Thermal Conductivity of a Three-Dimensionally Structured Fluid-Saturated Metal Foam," International Journal of Heat and Mass Transfer, **44**, pp. 827-836.
[9] Calmidi, V. V. and R. L. Mahajan, 1999, "The Effective Thermal Conductivity of High Porosity Fibrous Metal Foams," Journal of Heat Transfer-Transactions of the ASME, **121**, pp. 466-471.
[10] Paek, J. W., et al., 2000, "Effective Thermal Conductivity and Permeability of Aluminum Foam Materials," International Journal of Thermophysics, **21**, pp. 453-464.
[11] Weaire, D. and S. Hutzler, 1999, *The Physics of Foam*, Oxford, Clarendon Press.
[12] Unigraphics Solutions, Maryland Heights, Missouri.
[13] Structural Research and Analysis Company, Los Angeles, California.
[14] Kim, K. J., et al., 1998, "Development of Lani5/Cu/Sn Metal Hydride Powder Composites," Powder Technology, **99**, pp. 40-45.
[15] ERG, Materials and Aerospace Corporation, Oakland, California.